81

HIGH TEMPERATURE, HIGH PULSE POWER LITHIUM BATTERIES

H. F. GIBBARD

Power Conversion, Inc., 280 Midland Avenue, South Building, Saddle Brook, NJ 07662 (U.S.A.)

Summary

Studies have been carried out to increase the capability of high-temperature, molten-salt batteries to deliver pulses and bursts of electrical energy at high specific power. The performance of the lithium alloy–iron disulfide system, which can produce 1 - 10 ms pulses at 50 - 75 kW kg^{-1}, was taken as a baseline. Various materials having improved thermal stability and higher electrode potential have been evaluated as possible active materials *versus* lithium, and several alkali halide mixtures have been evaluated as electrolytes for high-current operation. Lithium cobalt oxide and lithium molybdenum sulfide showed the possibility for reversible operation but did not yield current densities adequate for high-power operation. Only lithiated vanadium oxide, a mixture of LiV_2O_5 and VO_2, showed the desired advantages over FeS_2: higher electrode potential, lower polarization at high current density, and improved thermal stability.

Introduction

Molten salt batteries operating at high temperature have the capability to deliver electrical energy at extremely high specific power. A method of attaining specific power approaching megawatts per kilogram of battery mass has been described [1]. High-temperature operation was proposed to circumvent kinetic limitations, and the use of highly conductive molten salt electrolytes in bipolar batteries was recommended to minimize polarization losses. Bipolar lithium–silicon/iron disulfide batteries were described which yielded a specific power of 50 - 75 kW kg^{-1} when discharged in pulses lasting 1 - 10 ms. The present paper describes research directed at increasing the maximum battery power achievable during high-rate discharge lasting up to a few minutes.

For bipolar batteries in which the only significant source of polarization is the ohmic resistance of the separator/electrolyte, the maximum power varies as the electrolytic conductivity, as the square of the open-circuit voltage, and inversely as the thickness of the separator/electrolyte [1]. Changes likely to improve specific power are thus: increasing the open-circuit cell voltage, increasing the conductivity of the electrolyte, and decreas-

ing the thickness of the separator/electrolyte. Taking the lithium(alloy)–iron disulfide bipolar battery as a baseline, we shall consider each of the three factors for performance improvement. Because of its high negative electrode potential, little increase can be gained in the open-circuit voltage by replacing lithium with another negative active material. Replacing the lithium alloys lithium–aluminum or lithium–silicon with elemental lithium immobilized in a metal matrix [2, 3] increases the open-circuit potential by 150 - 300 mV. It also avoids possible diffusional limitations in the solid at high current densities and long discharge times. A more promising approach to increasing the open-circuit voltage is replacement of iron disulfide with an active material having a more positive electrode potential.

While lithium and its useful alloys are near the negative voltage limit of alkali halide fused salts, the potential of the iron disulfide electrode lies about 1.5 V negative of the positive voltage limit of, for example, chloride melts. Accordingly, we have investigated alternative positive active materials including transition metal oxides, sulfides, selenides, and oxyhalide salts, as well as high-valent metal chlorides and fluorides. Metal oxides have been identified that, in addition to greater open-circuit voltage, exhibit much better thermal stability than iron disulfide, which decomposes rapidly above 550 °C. These include lithiated vanadium oxide [4] and chromium oxide [5]. Results in single-cell experiments on several of these compounds, which show promise for pulse battery applications, are described below.

Experiments have been carried out using several electrolytes with varying amounts of binder and thicknesses of the separator/electrolyte layer. The effects of these changes on the specific resistance per unit area of separator will be described.

Experimental

Materials

Lithium–silicon alloy was obtained as a -40 mesh powder, with a nominal composition of 44 wt.% lithium, from Lithium Corporation of America, Gastonia, NC. Magnesium oxide ("Maglite S") was obtained as a submicron powder from Whittaker, Clark & Daniels, South Plainfield, NJ.

Three electrolytes were obtained from Anderson Physics: LiCl–KCl eutectic electrolyte (45:55 wt.%, respectively), LiF–LiCl–LiBr (9.6:22:68.4), and LiCl–LiBr–KBr (12.1:36.5:51.4). Additionally, the all-lithium-cation mixture was prepared in-house from salts purchased from Lithium Corporation of America.

Iron disulfide obtained from EM Science, Cherry Hill, NJ, was dried at 50 °C under vacuum for 16 h and sieved to obtain the 250 - 325 mesh powder used in positive electrode fabrication. Lithium dioxycobaltate(III) ($LiCoO_2$) was obtained as a powder with approximately 1 μm particle size from Basic Volume Ltd., London, England. It was also synthesized in-house by the decomposition of cobalt(II) carbonate and lithium carbonate in the presence of oxygen [6]:

$$2CoCO_3 + Li_2CO_3 + \tfrac{1}{2}O_2 \longrightarrow 2LiCoO_2 + 3CO_2 \tag{1}$$
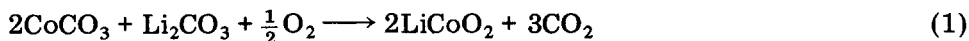
and by oxidation of cobalt(II) oxide by lithium peroxide [7]:

$$2CoO + Li_2O_2 \longrightarrow 2LiCoO_2 \tag{2}$$

Molybdenum(VI) oxide, lead(IV) fluoride, copper(II) chloride, and manganese(III) fluoride were obtained from Alfa Products, Danvers, MA, and were used as received. Molybdenum disulfide (MoS_2) was obtained as an ultrapure powder from Samin Corporation of New York, NY.

Lithiated vanadium oxide was prepared by the reaction of V_6O_{13} with lithium bromide in quartz boats under flowing argon at 600 °C [4]:

$$V_6O_{13} + LiBr \longrightarrow LiV_2O_5 + 4VO_2 + \tfrac{1}{2}Br_2 \tag{3}$$
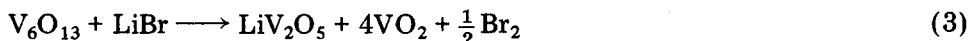
The nonstoichiometric V_6O_{13} required for this synthesis was obtained from the two-step thermal decomposition at 450 °C and 550 °C of ammonium metavanadate (NH_4VO_3) under flowing argon [8].

Preparation of negative electrode, separator–electrolyte, and positive electrode

The cell components were fabricated from the powdered constituents as thin discs or pellets by compression in cylindrical dies. The processing of the raw materials was carried out, according to procedures similar to those employed for thermal battery fabrication [9], in a dry room in which the relative humidity ranged between 1 and 3%.

In experiments in which the electrolyte was eutectic lithium chloride–potassium chloride, negative electrodes were composed of lithium–silicon alloy (nominal 44 wt.% lithium). In the work with other electrolytes the negative electrode contained 65 wt.% of the lithium–silicon alloy and 35 wt.% of electrolyte. The separator–electrolyte component was composed of 65 wt.% electrolyte and the balance of magnesium oxide powder.

The composition of the positive electrodes varied depending on the mechanical properties of the pellets and the need for conductive additives. Iron disulfide positives contained 80 wt.% FeS_2 and the balance of electrolyte. Cupric chloride positives contained 43 wt.% $CuCl_2$, 10 - 20 wt.% graphite powder, 13 wt.% electrolyte, and 25 - 35 wt.% magnesium oxide to prevent collapse of the pellet under the pressure applied to the test cell. Lithiated vanadium oxide positives contained 70 - 90 wt.% active material and the balance of electrolyte. Lithium cobalt oxide cathodes contained 50 wt.% $LiCoO_2$, the balance being electrolyte (15 - 25 wt.%) and graphite powder. Molybdenum(VI) oxide positives contained 60 wt.% MoO_3, with the balance of 20 wt.% each of electrolyte and graphite powder. Manganese(III) fluoride, lead(IV) fluoride, and molybdenum disulfide positives all contained 63 wt.% of the active component, 21 wt.% electrolyte and 16 wt.% graphite.

Cell tests

Cells were tested in a single-cell tester adapted from a design of Sandia National Laboratories [10]. Each pellet had a cross-sectional area of 2.85 cm^2.

A cell, consisting of a positive electrode, a negative electrode, and an intermediate separator–electrolyte pellet, was sandwiched between molybdenum foil current collectors. This cell assembly was placed between two aluminum platens which were thermostatically controlled within ±2 °C in the range 350 °C - 600 °C. Mica insulators separated the heated platens from the cell current collectors. The external pressure applied to the cell was adjusted by means of a weight placed on a pan connected to the upper platen. This ranged from 15 kPa to 155 kPa.

Cell voltage was monitored as a function of time using a Hewlett-Packard Model 7090 measurement plotting system. Cells were discharged, and in some cases charged, using a Hewlett-Packard Model 6023A power supply in the constant-current mode. Cell current was recorded on another channel of the H-P 7090 by measuring the voltage across a precision shunt in series with the cell.

Results

The results for the various positive active materials investigated are discussed individually. The ranges of compositions of the positive electrode pellets are given in the experimental section.

FeS$_2$. We have carried out a very large number of experiments on lithium alloy–iron disulfide cells and bipolar batteries. Only a few results which demonstrate some of the limitations of these batteries in high-power applications are presented here. Figure 1 shows the apparent specific impedance of single cells containing a lithium–silicon negative electrode and an LiF–LiCl–LiBr electrolyte, as a function of the thickness of the separator/electrolyte. These results were obtained on fully charged cells by a current-interruption technique. As expected, the apparent specific impedance was linear with separator thickness. Extrapolation to zero separator thickness yielded a specific impedance of 0.53 ohm cm^2. Tests on single cells with reference electrodes showed that three-quarters of the cell polarization, corrected for the resistance of the separator/electrolyte, was attributable to the positive electrode. The total apparent impedance of the cell decreased with increasing temperature, and this suggested operating at a higher temperature to increase the power capability.

Figures 2 and 3 illustrate the problems associated with operating iron disulfide cells at higher than normal temperature. At 500 °C (Fig. 2) the capacity of the cells to any normal cutoff voltage follows a regular progression with changing current density. At 550 °C, however, cells discharged at 0.5 A cm^{-2} and 1.0 A cm^{-2} yield about the same capacity, and cells discharged at 0.25 A cm^{-2} give the same capacity to a cutoff voltage of 1.3 V. The cause for this behavior is the well-known thermal instability of iron disulfide, which begins to decompose rapidly above 500 °C. These results show the need for a positive active material with improved thermal stability for operation at high power levels.
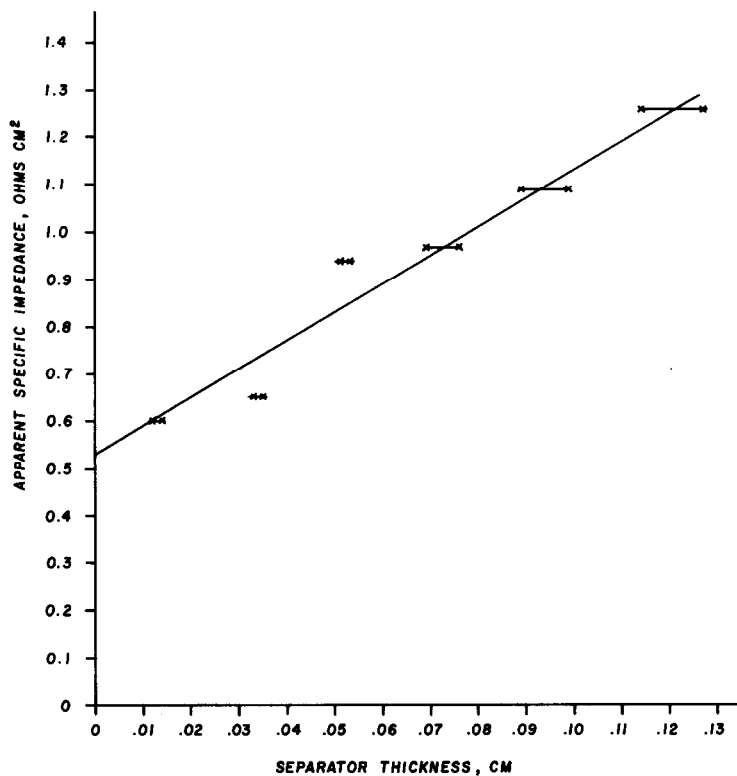
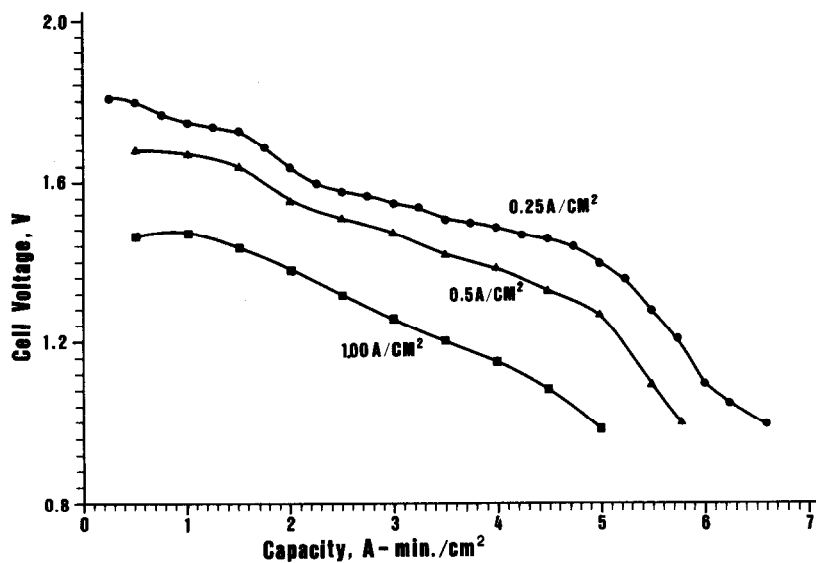Fig. 1. Apparent specific impedance of FeS_2 cells at 500 °C, as a function of separator thickness.

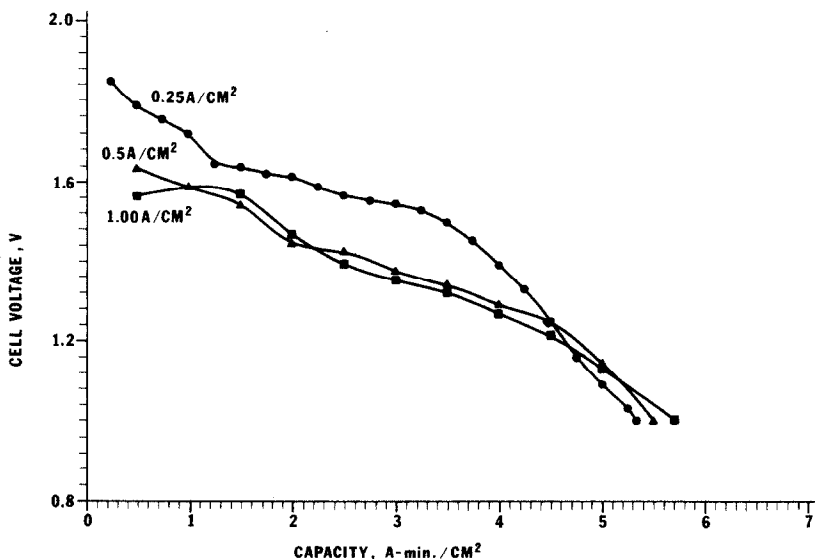Fig. 2. Cell voltage *vs.* capacity for discharge of FeS_2 cells at 500 °C.

Fig. 3. Cell voltage *vs.* capacity for discharge of FeS₂ cells at 550 °C.

MoS₂. Cells containing MoS_2 positive electrodes showed initial open-circuit voltages of 1.75 - 2.25 V, but in every case this rapidly dropped to a lower steady voltage which varied widely from cell to cell. The best cells maintained a voltage greater than 1.0 V at a current density of 0.2 A cm^{-2}.

CuCl₂. Seven different batches of cupric chloride positive active material were prepared. Those which yielded adequate mechanical strength when pressed into pellets were evaluated in the single-cell tester. The pellets with the best structural integrity were composed of 43 wt.% $CuCl_2$, 13 wt.% electrolyte, 9 wt.% graphite, and 35 wt.% MgO. Adequate pellets were also obtained from a mixture with 18 wt.% graphite and 26 wt.% electrolyte, the other components remaining constant. The performance of these two types of cathodes on polarization and capacity tests (see below) was essentially the same. The LiCl–KCl eutectic electrolyte was chosen so that a wide range of temperatures could be covered. The open-circuit voltage of these cells upon exposure to test temperatures in the range 400 °C - 500 °C was initially 2.8 V; over a period of minutes this declined to 1.9 - 2.2 V. After the voltage stabilized, a polarization curve for the cell was taken.

Figure 4 shows the results of polarization tests in which the voltage was read after 15 s at the constant current shown. At 400 °C and 450 °C the apparent internal resistance of the cells was high, and evidence for activation polarization was seen. At 500 °C the behavior was ohmic, and the apparent specific impedance was 0.93 ohm cm^2. At current densities of 500 mA cm^{-2} or more, however, the voltage declined if the current was maintained for more than 10 - 15 s.
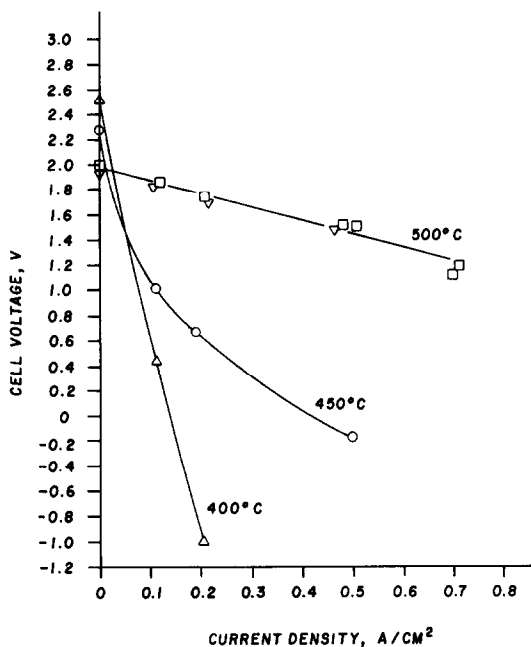
Fig. 4. Polarization curves for CuCl$_2$ at various temperatures.

The electrochemical capacity of the cupric chloride pellets was determined by discharge at 50 mA cm^{-2}. The theoretical capacity was 28.7 mA h cm^{-2}, based on one-electron reduction. The utilization upon discharge to zero cell voltage was 55 - 60% at 450 °C and at 500 °C.

MnF$_3$ and PbF$_4$. Several positive active materials were made up using MnF$_3$ and PbF$_4$, graphite, and eutectic LiCl–KCl electrolyte. It was anticipated that these high-valent metal fluorides would oxidize chloride ion in the melt to chlorine, and that it would be possible to reduce the chlorine at a high potential. The first expectation was realized, but the second was not. Upon heating to 365 °C the cells showed voltages of more than 3.4 V, which rapidly decayed with time. A discharge current of 100 mA cm^{-2}, the lowest current density of interest in this study, drove the cells deeply into voltage reversal. Porous carbon was added to the positive electrode mix to stabilize the potential of the cells by adsorption of chlorine. The potential stabilized almost immediately at about 2.2 V, but the cells did not produce a positive potential under useful discharge current densities.

LiCoO$_2$. The LiF–LiCl–LiBr electrolyte was used in experiments with LiCoO$_2$. It was found necessary to pre-fuse and then grind mixtures of the active material, graphite and electrolyte at 650 °C in order to obtain material which could be pressed into pellets. The open-circuit voltage of cells on raising the temperature to 500 °C varied from slightly under 1.6 V to 2.1 V.
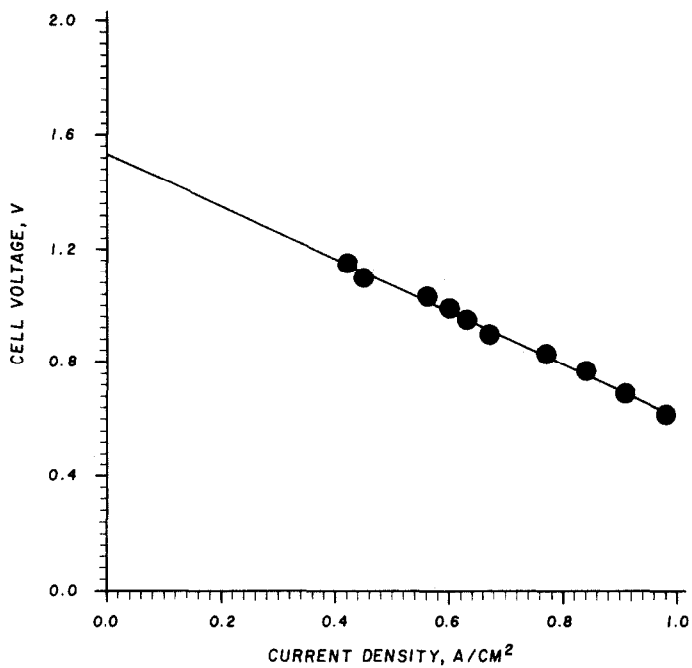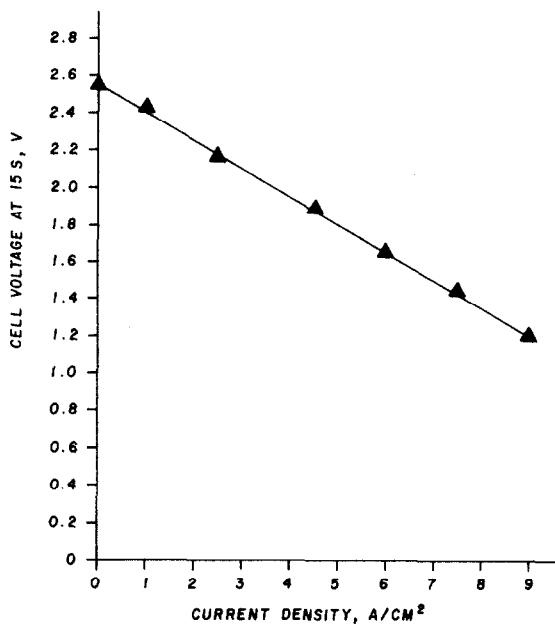
Fig. 5. Polarization curve for $LiCoO_2$ at 500 °C.

Fig. 6. Polarization curve for lithiated vanadium oxide at 577 °C.

The polarization curve, *e.g.*, Fig. 5, was linear within experimental error. Cells with $LiCoO_2$ positives were rechargeable up to a maximum OCV of slightly more than 1.8 V. The coulombic efficiency of cells cycled five times at current densities of 0.25 A cm^{-2} - 0.50 A cm^{-2} averaged only 56%.

Lithiated vanadium oxide. The best performance of lithiated vanadium oxide cells using LiF-LiCl-LiBr electrolyte was obtained at 577 °C, as shown by the polarization curve, Fig. 6. Because each test removed a significant amount of capacity, each point represents the performance of a fresh, fully charged cell. The open-circuit voltage of the cells was stable to within a few millivolts over a 10 min period. The specific power of these cells, calculated on the basis of the active materials alone, is shown in Fig. 7. These results are not directly comparable with the performance of the FeS_2 cell during pulse tests of millisecond duration [1], since the duration of current flow is more than a factor of 1000 greater in the present results. FeS_2 cells tested at 500 °C under a current density of more than 5 A cm^{-2} exhibit negative terminal voltage.
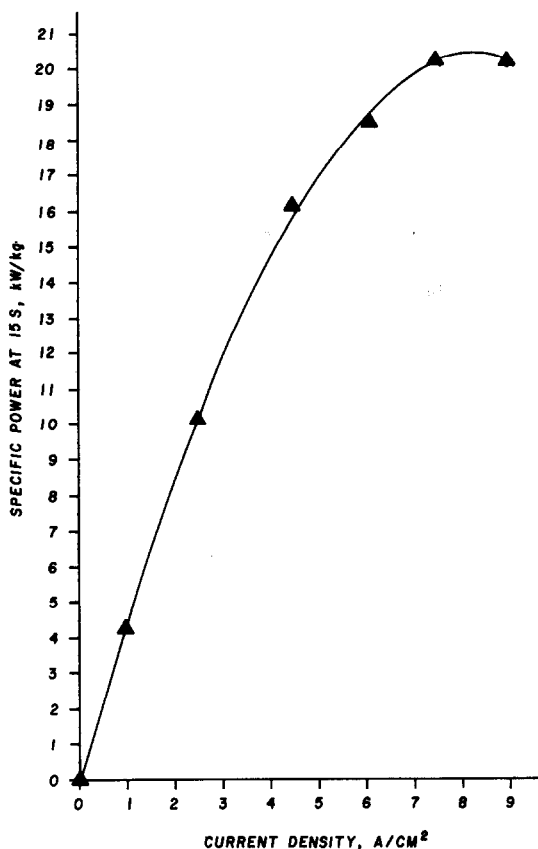

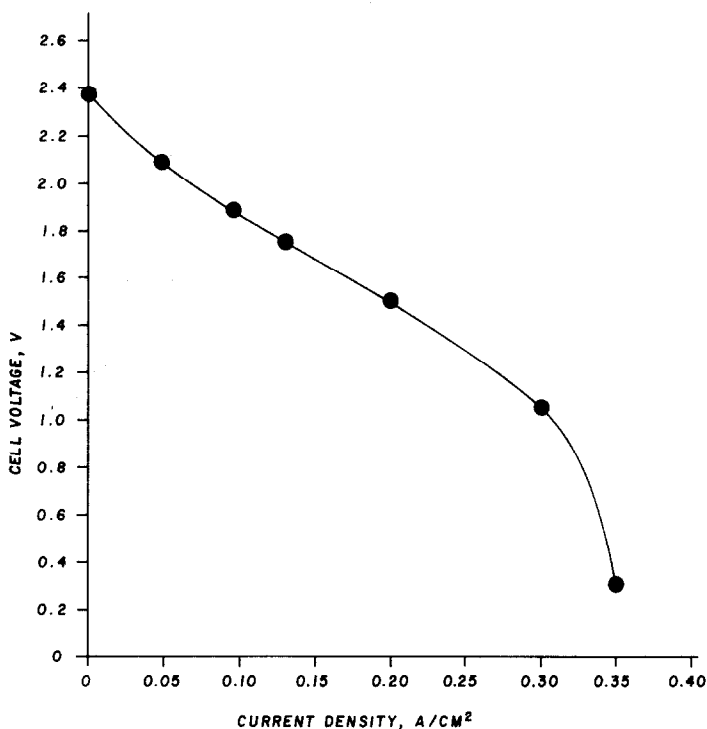Fig. 7. Specific power of lithiated vanadium oxide cells at 577 °C *vs.* current density.

Fig. 8. Polarization curve for MoO_3 at 500 °C.

MoO_3. Cells containing molybdenum oxide positive electrodes showed the relatively high initial open-circuit voltage of about 2.4 V, but their internal impedance was high, as shown in Fig. 8.

Discussion

Three materials showed some promise for use in high-specific-energy, high-temperature batteries: $CuCl_2$, $LiCoO_2$, and lithiated vanadium oxide. Cupric chloride showed no significant advantages over iron disulfide up to temperatures of 500 °C, and above that temperature both materials showed evidence of thermal instability.

$LiCoO_2$ had been under evaluation in our laboratory as a positive active material in ambient-temperature, organic-electrolyte, rechargeable lithium batteries. In this application, cell voltages of up to 4 V had been found for fully charged cells, *i.e.*, cells in which x in the reaction

$$LiCoO_2 \longrightarrow (1-x)\,Li + Li_x CoO_2$$

is near zero. On the basis of these results it might be expected that $LiCoO_2$ would be a powerful oxidant in the molten salt, with a potential near the chlorine evolution potential. In fact, the material could not be charged above

an open-circuit potential of 1.82 V. This is in close agreement with the results of Godshall *et al.* [11] who found an intrinsic limit of 1.82 V for transition metal oxides in LiCl–KCl eutectic electrolyte. The relatively low cell potential rules out $LiCoO_2$ for extremely high-power applications.

Lithiated vanadium oxide shows promise of surpassing iron disulfide for use in high-power, molten salt batteries. It exhibits better thermal stability and less polarization during prolonged discharge at high current density.

The limiting source of polarization in lithium alloy–iron disulfide batteries was found to be electrode polarization, particularly that of the positive electrode. No limit to the increase in conductance of the separator/electrolyte with decreasing separator thickness was found, down to thicknesses of 0.01 cm. Thus, our search for high-temperature systems which yield higher specific power will continue to concentrate on electrodes with extremely rapid kinetics and low diffusion overvoltage.

Acknowledgement

References

1 H. F. Gibbard, in J. R. Selman and H. C. Maru (eds.), *Electrochemical and Thermal Modeling of Battery, Fuel Cell, and Photoenergy Conversion Systems, Proc. Vol. 86-12,* The Electrochemical Society, Pennington, NJ, 1986, pp. 193 - 205.
2 C. S. Winchester, in *Proc. 30th Int. Power Sources Symp.*, The Electrochemical Society, Pennington, NJ, 1982, pp. 23 - 26.
3 M. T. Williams, C. Winchester and J. Jolson, in *Proc. 32nd Int. Power Sources Symp.*, The Electrochemical Society, Pennington, NJ, 1986, pp. 658 - 663.
4 I. Faul, in *Proc. 32nd Int. Power Sources Symp.*, The Electrochemical Society, Pennington, NJ, 1986, pp. 636 - 642.
5 D. K. McCarthy, F. M. Delnick and R. A. Guidotti, *U.S. Pat. 4,508,796*, April, 1985.
6 K. Mizushima, P. C. Jones, P. V. Wiseman and J. B. Goodenough, *Mater. Res. Bull., 15* (1980) 783.
7 W. D. Johnston, D. R. Heikes and D. Sestrich, *J. Phys. Chem. Solids, 7* (1958) 1.
8 D. W. Murphy, P. A. Christian, F. J. DiSalvo, J. N. Carides and J. V. Waszcarh, *J. Electrochem. Soc., 128* (1981) 2053.
9 H. K. Street, Characteristics and development report for the MC3573 thermal battery, *SAND82-0695*, Sandia National Laboratories, February, 1983.
10 D. M. Bush, Thermal battery cell testing: apparatus and results, *SLA 73-0896*, Sandia National Laboratories, Albuquerque, December, 1973.
11 N. Godshall, I. D. Raistrick and R. A. Huggins, *J. Electrochem. Soc., 131* (1984) 543.